Original Article

External Arrhythmia Ablation Using Photon Beams
Ablation of the Atrioventricular Junction in an Intact Animal Model

H. Immo Lehmann, MD; Amanda J. Deisher, PhD; Mitsuru Takami, MD; Jon J. Kruse, PhD; Limin Song, PhD; Sarah E. Anderson, PhD; Jack T. Cusma, PhD; Kay D. Parker, CVT; Susan B. Johnson, BS; Samuel J. Asirvatham, MD; Robert C. Miller, MD; Michael G. Herman, PhD; Douglas L. Packer, MD

Background—This study sought to investigate external photon beam radiation for catheter-free ablation of the atrioventricular junction in intact pigs.

Methods and Results—Ten pigs were randomized to either sham irradiation or irradiation of the atrioventricular junction (55, 50, 40, and 25 Gy). Animals underwent baseline electrophysiological evaluation, cardiac gated multi-row computed tomographic imaging for beam delivery planning, and intensity-modulated radiation therapy. Doses to the coronary arteries were optimized. Invasive follow-up was conducted ≤4 months after the irradiation. A mean volume of 2.5±0.5 mL was irradiated with target dose. The mean follow-up length after irradiation was 124.8±30.8 days. Out of 7 irradiated animals, complete atrioventricular block was achieved in 6 animals of all 4 dose groups (86%). Using the same targeting margins, ablation lesion size notably increased with the delivered dose because of volumetric effects of isodose lines around the target volume. The mean macroscopically calculated atrial lesion volume for all 4 dose groups was 3.8±1.1 mL, lesions extended anteriorly into the interventricular septum. No short-term side effects were observed. No damage was observed in the tissues of the esophagus, phrenic nerves, or trachea. However, histology revealed in-field beam effects outside of the target volume.

Conclusions—Single-fraction doses as low as 25 Gy caused a lesion with interruption of cardiac impulse propagation using this respective target volume. With doses of ≤55 Gy, maximal point-doses to coronary arteries could be kept <7Gy, but target conformity of lesions was not fully achieved using this approach. **(*Circ Arrhythm Electrophysiol*. 2017;10:e004304. DOI: 10.1161/CIRCEP.116.004304.)**

Key Words: atrioventricular node ■ catheter ablation ■ photons ■ tachycardia, ventricular ■ x-ray

Catheter ablation has emerged as the primary treatment modality for several different cardiac arrhythmias. However, catheter ablation in many arrhythmias has limitations that could be overcome by noninvasive ablation using external beam therapies. Even though noninvasive[1] and intraprocedural imaging and mapping techniques[2] have dramatically improved the anatomic assessment of the ventricular arrhythmia substrate, catheter ablation offers limited success rates.[3] Often, this is because of the limited tissue penetration depth of applied energy sources.[2,4,5] In addition, catheter-ablation is associated with many different risks such as thromboembolic events,[6,7] pulmonary vein stenosis, and atrial–esophageal fistula formation.[8,9]

Invasive delivery of ionizing radiation to distinct cardiac locations has shown that myocardial lesion creation with this energy source is feasible.[10–12] Noninvasive delivery of photons using the CyberKnife system has lately created incentive for a completely noninvasive arrhythmia ablation approach[13] and has recently been performed as a first-in-man treatment.[14] Similarly, sophisticated photon beam deliveries, such as intensity-modulated radiation therapy, have gained good ability to focus relatively high irradiation doses, required for cardiac ablation, into small target volumes. In addition, linear photon dose fall-off in the tissues makes these beams relatively robust in the presence of complex target motion. This study sought to ablate the atrioventricular junction completely noninvasively, using a single-fraction, image-guided application of photon beams in an intact porcine model.

Methods

Study Design

Ten domestic healthy pigs (*sus scrofa domestica*) of either sex were included at 10 weeks of age and randomized to irradiation of the atrioventricular junction with doses of 25, 40, 50, and 55 Gy. All animal procedures were approved by Mayo Clinic's institutional

Received October 13, 2016; accepted March 6, 2017.

From the Mayo Clinic Translational Interventional Electrophysiology Laboratory (H.I.L., M.T., K.D.P., S.B.J., S.J.A., D.L.P.) and Department of Radiation Oncology (A.J.D., J.J.K., L.S., S.E.A., J.T.C., R.C.M., M.G.H.), Mayo Clinic, Rochester, MN; and Texas Center for Proton Therapy, Irving (L.S.).

Guest Editor for this article was Gerhard Hindricks, MD.

Correspondence to Douglas L. Packer, MD, Mayo Clinic, Saint Marys Hospital, 2–416 Alfred Bldg, Rochester, MN 55902. E-mail packer@mayo.edu

WHAT IS KNOWN

- Sophisticated external x-ray therapies allow relatively focused delivery of ionizing radiation in cancer therapy.
- Image-guided delivery of x-rays to myocardium is of interest for noninvasive ablation of arrhythmias.

WHAT THE STUDY ADDS

- Intensity-modulated radiation therapy can be relatively precisely focused to the atrioventricular junction to noninvasively achieve complete atrioventricular block despite cardiac and respiratory motion.
- Complete atrioventricular block can be achieved with relatively small x-ray doses, and increasing dose increases lesion size.

animal care and use committee and performed in full compliance with its guidelines.

Anesthesia and Monitoring During Surgical Procedures

Anesthesia was induced using an IM dose of telazol (4.4 mg/kg), ketamine (2.2 mg/kg), and xylazine (2.2 mg/kg). After intubation, animals were ventilated on 1% to 3% isoflurane and monitored using 4 surface ECG electrodes, invasive blood pressure, temperature, and Spo_2.

Sedation and Positioning During Computed Tomographic Imaging and Photon Irradiation

During cardiac imaging and photon beam irradiation, animals were sedated using a continuous IV drip of propofol (10 mg/mL; 0.25–0.30 $mg \cdot kg^{-1} \cdot min^{-1}$) without additional paralytic use. Animals were immobilized using a vacuum cushion (BodyFIX BlueBAG; ElektaAB, Stockholm, Sweden) to ensure a stable, reproducible position for computed tomographic (CT) imaging and radiation therapy delivery. The CT reference point (CT laser system) was marked on the skin and on the cushion.

Specific Methods

The specific methods, including electrophysiological study and treatment planning CT acquisition, were conducted as recently described using carbon ion (^{12}C) beams.[15]

Baseline Study and Electrophysiological Evaluation

The surgical field was shaved and prepped with povidone–iodine solution. A cut-down with subsequent vessel preparation for placement of introducer sheaths in the left/right external jugular vein and right/left femoral arteries and veins was performed. For intracardiac echocardiography, a 10F 5.5 to 10 MHz probe was used (Acuson; Cypress, Mountain View, CA). A 7F decapolar catheter was placed in the coronary sinus. Catheterization was performed under biplane fluoroscopic guidance. Electroanatomical mapping was performed (Carto XP, Biosense Webster, Inc, Diamond Bar, CA). A Navistar or Navistar-Thermocool mapping catheter was used (Biosense Webster). For each chamber, ≈200 points were sampled, and a fill-threshold <15 mm was considered as adequate to reflect a high-density map. Bipolar signals were recorded between the distal electrode pairs. Signals were displayed and recorded using a digital amplifying and recording system (CardioLab Electrophysiology Recording System, GE Healthcare). Left ventricular function was assessed using left ventricular ventriculography and intracardiac echocardiography. Intracardiac fiducials were implanted at the coronary sinus ostium, right atrial appendage, and left atrial appendage for biplane x-ray and cone beam CT positioning before irradiation (Quick Clip 2; 8×2 mm; Olympus, Shinjuku, Japan).[16]

Pacemaker Implantation

All animals underwent pacemaker implantation at the end of the baseline electrophysiological evaluation. After removal of the sheath from the external jugular vein, two 7F active fixation pacing leads were introduced through 2 small incisions in the vessel wall. Atrial leads were placed in the right atrial appendage, and right ventricular leads were placed in the right ventricular apex. Leads were tunneled and connected to a pacemaker unit placed in a subcutaneous postauricular pocket (Medtronic, Inc, Minneapolis, MN).

Treatment Planning CT Acquisition

Cardiac-gated native and contrast-enhanced CT scans were acquired for photon beam treatment planning on a 64 row Siemens Somatom Definition Flash scanner (Siemens Healthcare, Forchheim, Germany). Contrast-enhanced scans were obtained after injection of 50 mL contrast agent (4 mL/s; 8–10 seconds delay; Omnipaque 350 mg I/mL; GE Healthcare) through a cannula in a branch of the caudal auricular vein. All scans were acquired at expiration using a pause of the respirator. Ten cardiac phases with 1 mm voxel and slice spacing were reconstructed with an enhanced field of view of 400 mm for skin-to-skin images required for radiotherapy planning.

Contouring and IMRT Treatment Planning

A sphere of 5 mm diameter was contoured as atrioventricular junction ablation lesion on all 10 cardiac phases. The average contour position was subsequently transferred into the phase-averaged CT scan that was used for all subsequent treatment planning steps. Organs at risk for beam delivery were contoured on the averaged CT as well. All treatment planning was conducted using Eclipse (Varian Medical, Palo Alto, CA) treatment planning software. Cardiac motion was incorporated by anisotropic expansion of the target (±1 mm left–right, ±4 mm superior–inferior, and±4 mm anterior–posterior). In addition, a margin of±4 mm was added for positional uncertainty and residual respiratory motion. All treatment plans were computed using 2 or 3 arcs. Dose restrictions from single-fraction x-ray deliveries were used for treatment plan computation; restrictions to coronary arteries were included into the dose optimization process.[17]

Animal Repositioning and Photon Irradiation of the Atrioventricular Junction

At the time of treatment, animals were initially aligned in the BodyFIX bag using an in-room laser system and skin markings. Subsequently, isocenter position was refined using matching of bony anatomy in 2 digitally reconstructed radiographs derived from the CT scan compared with 2 orthogonal in-room x-ray images. The match was finalized using position of the CS ostium fiducial clip on in-room (cone beam) CT, conducted during expiration and inherently averaged during the cardiac cycle. Beam delivery of 6 MV photons was gated to expiration and was performed using a linear accelerator (True Beam; Varian Medical).

Follow-Up After Irradiation

Animals were followed for ≤16 weeks after irradiation. Device interrogations were performed after 4, 8, and 12 weeks and at termination of follow-up where the animals also underwent a procedure identical to the one conducted at baseline as described above. Animals were euthanized through induction of ventricular fibrillation directly followed by exsanguination.

Pathological Examination

Heart, lungs, trachea, phrenic nerves, and esophagus were removed en bloc with the pericardium intact. Triphenyltetrazolium chloride

(Sigma Aldrich, St Louis, MO) was used to delineate the ablation lesions. Gross pathological findings were assessed, and all macroscopically visible lesion dimensions were measured on the endocardial surface in the nonfixed tissue. Lesion volumes were calculated as described in infarcted tissue.[18]

Histological Examination

For histological analysis, samples were fixed in 10% formaldehyde and processed. After fixation, samples were wax embedded and cut with a microtome. Cut sections (5μm) were stained with hematoxylin and eosin and Masson trichrome staining and evaluated using light microscopy.

Statistical Analysis

All statistical analyses were performed using SPSS 18. Baseline characteristics in Table 1 are depicted as mean±SD. Treatment planning data in Table 2 is depicted per individual case. Spearman correlation was used for bivariate correlations between the administered dose, the lesion area in electroanatomical mapping, and the calculated lesion volume. Isodose lines were correlated with electroanatomical lesion findings and macro and microscopic lesion outcomes. Median time to complete atrioventricular block was estimated using the Kaplan–Meier estimation model, treating the animal that died prematurely as censored observation. A P value <0.05 was used as cutoff value to indicate statistical significance.

Results

General Characteristics

Out of 10 animals, 2 animals were treated with a prescription dose of 55 Gy, 1 animal received 50 Gy, 2 animals received 40 Gy, and 2 animals were treated with 25 Gy. General characteristics of all animals are shown in Table 1. The mean animal weight at baseline was 31.7±2.7 kg. The mean follow-up duration was 120.7±7 days. The mean weight gain during the course of the follow-up was 61.1±5.2 kg. The mean left ventricular ejection fraction at baseline was 70±5%.

Contouring and Treatment-Planning Outcomes

Figure 1 depicts contouring outcomes used for subsequent treatment plan computation, including the target as well as cardiac and surrounding risk structures. The atrioventricular junction ablation lesion was contoured in the superior portion of the triangle of Koch. The mean volume receiving the prescription dose for atrioventricular junction ablation was 2.5±0.5 mL (including blood; Table 1) after target motion and tissue deformation was included. The maximal point doses per individual case to the coronary arteries, esophagus, trachea, and skin are depicted in Table 2. Figure 2 shows 3 actual treatment-planning outcomes for delivery of 55, 40, and 25 Gy to the atrioventricular junction in 3 planes. Restriction of the maximal allowed point dose to the coronary arteries led to a dose distribution that did not have perfect conformity with the target volume, producing relatively high doses anterior to the target volume.

Photon Beam Delivery

The mean irradiation time for all groups was 14.3±2.8 minutes (Table 1). Beam delivery for all animals was gated to the expiration phase of the respiratory cycle with a mean duty cycle of 60%.

Electrophysiology and Outcomes After Irradiation

The median time until complete atrioventricular block occurrence was 11.2 weeks (SE: 0.490) post-irradiation and developed in 6 out of 7 animals (86%; 1 animal [25 Gy] died prematurely of device-related infection and could not be evaluated in a similar fashion). For in vivo characterization of the lesion size that led to atrioventricular block, electroanatomical mapping was conducted. Results of electroanatomical mapping are shown in Figure 3. The size of the endocardial surface area without electrogram positively correlated to the administered dose (r_s=0.971; P=0.001; Figures 3 and 4). Complete atrioventricular block was persistent in all animals; in case of the animal treated with 25 Gy, block occurred during the follow-up study of this animal during mapping of the atrioventricular junction.

Macroscopic Lesion Outcomes and Correlation to Dose

The positive correlation of macroscopic lesion outcomes with the mapped area and the administered target dose is shown in Figure 4. Bivariate analysis revealed a positive correlation of r_s=0.971; P=0.001, for the calculated macroscopic lesion volume and administered dose. An exemplary macroscopic lesion, consisting of macroscopic visible fibrosis in the right atrial target region is shown in Figure 5A. In addition, isodose line extension led to lesion development in the septal left atrium (Figure 5B). The mean right atrial lesion volume

Table 1. Baseline and Follow-Up Characteristics of All 10 Animals Included Into the Analysis

	All Pigs (n=10)	Sham Control (n=3)	AVJ 25 Gy (n=2)	AVJ 40 Gy (n=2)	AVJ 50 Gy (n=1)	AVJ 55 Gy (n=2)
Mean weight at imaging, kg	32.02±3.6	32.5±4.6	31±3	34±2	28	30.4±0.4
Mean weight at irradiation, kg	32.5±3.8	…	32±4	33±2	29	31.4±0.4
Mean duration of follow-up, d	124.8±30.8	18.7±5.6	111	125±0	82	138±13
Mean time from CT to irradiation, d	4.3±1.6	…	6±1	5±0	3	2.5±0.5
Target contour diameter (CTV), cm	0.5	…	0.5	0.5	0.5	0.5
Volume receiving target dose, mL	2.5±0.5	…	2.8±0.2	2.0±0.4	1.9	2.8±0.1
Setup time (first image to beam), min	33.0±11.7	…	36.0±15.8	24.3±0.9	49.4	30.6±1.8
Irradiation time (beam on to beam off)	17.2±6.3	…	9.9±0.5	14.7±2.0	19.9	25.7±0.3
Total procedure time	50.2±13.5	…	45.9±16.2	39.0±2.9	69.3	56.3±2.1

Table 2. Resulting Mean Doses to Organs at Risk From Treatment Planning for Atrioventricular Junction Ablation

Case No.	Dose, Gy	Maximum Dose in Target	LCA, Gy	RCA, Gy	Trachea, Gy	Skin, Gy	Esophagus, Gy
1	55	60.7	6.8	6.0	14.1	13.4	12.6
2	55	60.4	7.1	6.5	15.3	12.7	11.4
3	50	53.5	9.5	9.0	9.2	9.7	7.7
4	40	45.7	4.7	4.3	11.1	10.3	9.6
5	40	44.8	4.6	4.0	13.0	8.3	9.8
6	25	28.9	2.7	2.3	7.0	4.8	5.2
7	25	29.2	2.7	2.3	7.9	5.8	6.3

Doses are stated for all organs at risk. Only the coronary arteries had to be included into the beam and dose optimization process. Included are only treated, but not sham-animals. In the 50 Gy case, a less strict threshold was applied for protection of the coronary arteries from dose. LCA indicates contour encasing the left anterior descending and the circumflex coronary arteries; and RCA, right coronary artery.

on pathological analysis for all dose groups was 3.8±1.1 mL. The mean right atrial lesion volume in the 55 Gy group was 5.1±2.9 mL. The mean right atrial lesion volume in 40 Gy was 3.0±1.0 mL and in 25 Gy was 2.6 mL. In case of 55 and 40 Gy animals, concordantly to the treatment-planning outcomes, lesions extended anteriorly into the right ventricle and interventricular septum. The mean maximal width of lesion extension into right ventricular myocardium was 17.2±9.1 mm.

Lesion Histology

Target Histology

Target tissue analyzed after 3 months of follow-up revealed dense fibrosis, present in the target tissue in all animals of all dose groups (Figure 5C and 5D). Similarly and consistent with macroscopic pathology, fibrosis extended anteriorly to the contoured area into the interventricular septum in all 3 dose groups.

Short-Term Toxicity

No collateral damage was observed in the esophagus, trachea, or other organs at risk. The myocardium of the coronary sinus was also spared in all cases. Coronary arteries did not show a reaction within 3 months of follow-up. No radiation-induced side effects were observed during 4 months of follow-up. The left ventricular ejection fraction did not change during follow-up between sham and irradiated animals (Table 2).

Discussion

Main Findings

In this study, we ablated the atrioventricular junction catheter-free using a 6 MV photon beam. Doses of 25 to 55 Gy created lesions that subsequently led to complete atrioventricular conduction block. Point doses to the coronary arteries were optimized to stay <10 Gy, and accordingly, ablation lesions were not fully target conformal. Lesion volumes positively correlated with isodose line spread around the target volume and increased with the administered target dose, despite the use of the same targeting margins in each dose group. Targeted tissue revealed dense fibrosis. Fibrosis was not present in myocardium of beam entry channels, however, histology revealed evidence of cardiomyocyte apoptosis in these areas.

External Photon Beam Radiation for Catheter-Free Ablation

In these presented chronic intact animal studies, photon beams could be appropriately focused for atrioventricular node ablation. Similar to our data with carbon ions (^{12}C), reliable ablation

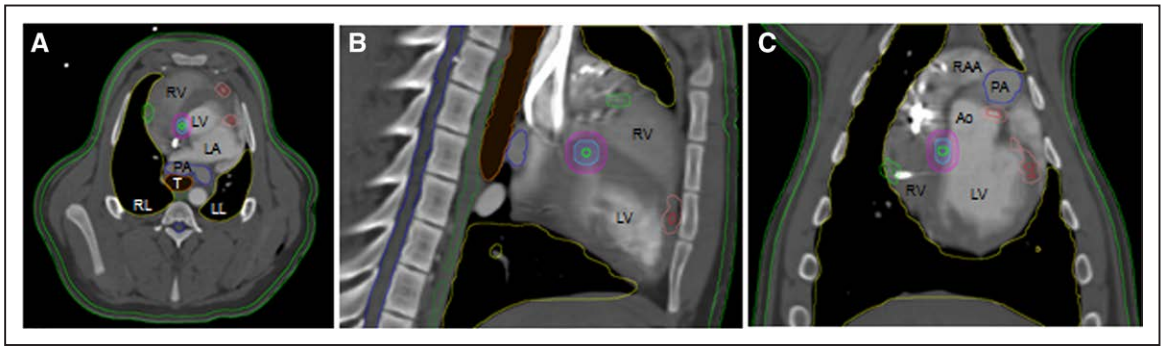

Figure 1. Contouring outcome for ablation of the atrioventricular junction in 3 planes of the cardiac phase-averaged computed tomographic (CT) scan. **A**, Axial (**B**) sagittal, and (**C**) coronal views. The ablation target contour (clinical target volume [CTV]) is depicted in green and was the average of 2 physicians'contours during 10 cardiac phases. The enhanced target contour, covering the amplitude of cardiac motion is shown in light blue (internal target volume [ITV]). Finally, the final target volume (planning target volume [PTV]) is shown in magenta. Yellow=lungs; orange=trachea; blue=pulmonary arteries; red=left coronary arteries; green=right coronary artery; light green=skin; and dark blue=spinal canal. Note that coronary arteries are enhanced by a 5-mm margin to form protected risk volume [PRV]. By limiting the dose to the PRV in the optimizer, the dose to the coronary arteries is robust to positional uncertainties.

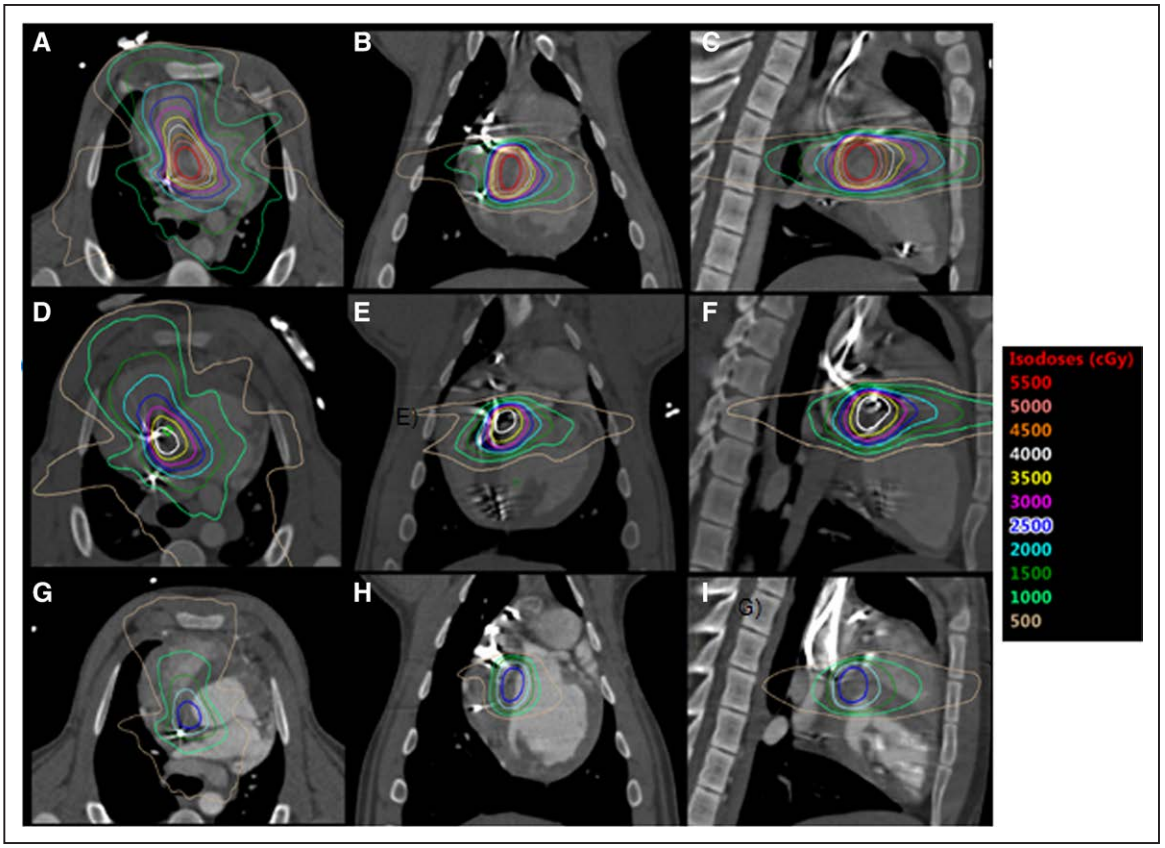

Figure 2. Treatment-planning outcomes for 3 different doses for irradiation of the atrioventricular junction. Note that the lower dose does not conform to the target volume because the dose restrictions to the coronary arteries were given high priority in the optimizer. This choice led to relatively high doses in the interventricular septum. **A**, Axial view, (**B**) sagittal view, and (**C**) coronal view for the 55 Gy administration. Following images depict 40 and 25 Gy with views in the same order. LA indicates left atrium; LAA, left atrial appendage; LL, left lung; LV, left ventricle; RA, right atrium; RL, right lung; RSPV, right superior pulmonary vein; and RV, right ventricle.

was achieved with 40 Gy. This study illustrates the biophysics of photon beams; the ultimate lesion size will depend on the irradiated target volumes, that is, the target dose and optimization constraints that will shape the dose distribution. Previous studies using the CyberKnife photon accelerator indicated that a dose as low as 25 Gy of photons may create an electrophysiological effect.[13,19–21] Our here-presented data support this finding for the here-irradiated volume, in which 25 Gy caused a lesion. The time frame for development of atrioventricular block in this study was similar to the CyberKnife studies and faster than what we have observed with ^{12}C beams.

Irradiation of a Moving Target With External Photon Beams

Even though photon beams are robust in the presence of target motion, considerable efforts needed to be undertaken in this study to guarantee dose delivery in the presence of contractile target motion; the approach used in this study was to expand the target volume to cover the whole amplitude of contractile motion, a method used for the treatment of mobile tumors in radiation oncology.[22] This conservative approach was chosen to ensure full coverage of the target with the prescription dose, thus allowing investigation of the required dose to achieve the desired ablation effect in the respective target volume. We are well aware of this limitation for the clinical application and are planning to use different techniques such as gating of the photon beam to the ECG as next steps to decrease the required irradiation margin size. Respiratory motion could already be well mitigated with an acceptable efficiency by using gating of the beam to the expiration phase of the respiratory cycle.

Photon Beams Versus Particle Beam Sources

This study illustrates how sparing of risk structures (eg, coronary arteries) is possible using photon beams, but how this also leads to higher doses at another location, explaining the observed anterior lesion extension into the interventricular septum. In this study, the volume irradiated with high and low doses of photons is larger than that in our study using ^{12}C particle beams. This translated into not only a greater lesion size but also greater involvement of myocardium located in the beam entry channels. This is because of the different physical properties of these 2 energy sources and the chosen beam arrangements. In photon beam radiation therapy, multiple beam angles are used to concentrate dose in the target region where the beams overlap and distribute the entry and exit dose of beam, leading to a larger myocardial volume receiving low-dose radiation. For the plans in this study, each arc comprised 178 distinct photon beams. The long-term effects for lesions creation and of exposure of these larger myocardial volumes in comparison to the different forms of particle therapies

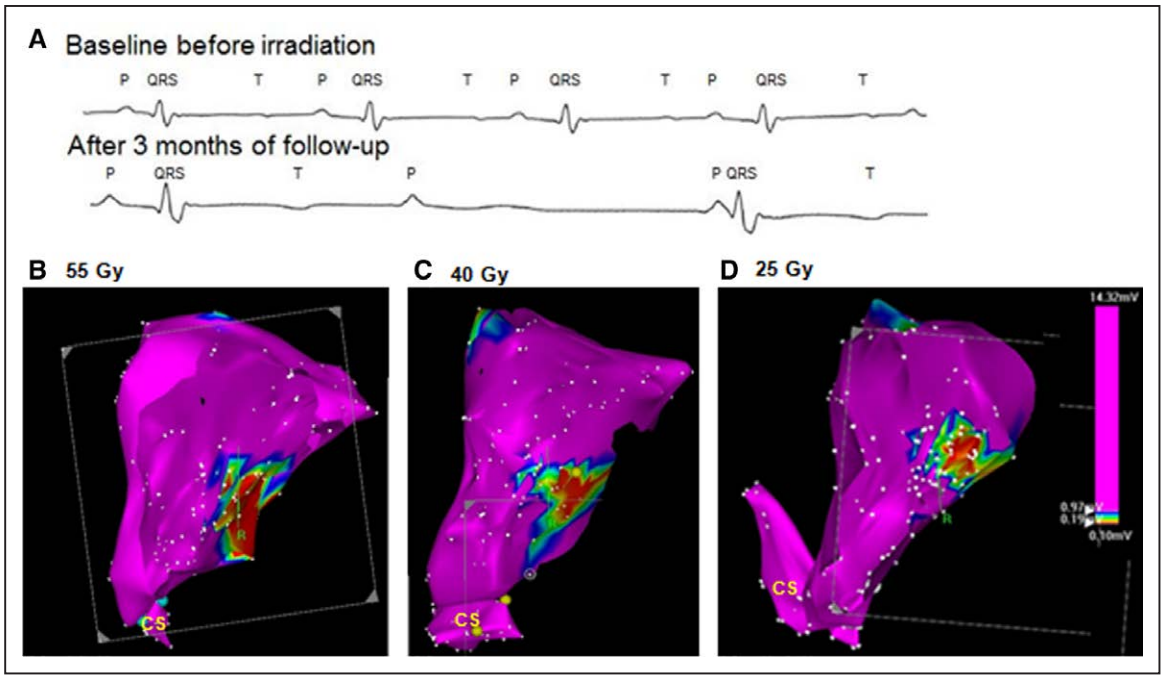

Figure 3. A, **Top**, Surface ECG at baseline before irradiation, showing sinus rhythm. **Bottom**, Three months after irradiation with 50 Gy, development of complete atrioventricular block with dissociation of atrial and ventricular activity. **B**, Right lateral view of the septal site of endocardial voltage maps 3 mo after irradiation with 55, 50, 40, and 25 Gy for electroanatomical lesion characterization. All animals had complete atrioventricular block present at the time of mapping. The coronary sinus is marked. Voltage thresholds as depicted on the color bar on the right-hand side.

(H^+, ^{12}C, ^{4+}He) need to be investigated in future studies with much longer follow-up times after the irradiation.

Study Limitations

First, the number of animals that was included into this study was limited. Second, anatomy and position of risk structures in the porcine heart is different than in men, but nevertheless the porcine heart is an accepted model for cardiac arrhythmia ablation. Third, doses in human tissue might be different and among other factors, will be dependent on the finally irradiated myocardial volume and the irradiated myocardial location. Fourth, intracardiac markers were implanted for verification during cardiac matching. However, using in-room CT for animal repositioning at the time of irradiation, these were rarely necessary for finding a good match (unpublished data). Fifth, size of the used margins for cardiac motion and position error cannot be 1:1 transferred to the clinical application. Our group is working on several approaches to downsize required margin size. Last, ionizing radiation has long-term side effects that need to be evaluated for this technology in risk-benefit modeling and long-term follow-up studies.

Clinical Implications

Arrhythmia ablation without the use of catheters has pertinent clinical implications. After we have performed these initial atrioventricular node ablation studies, we have successfully

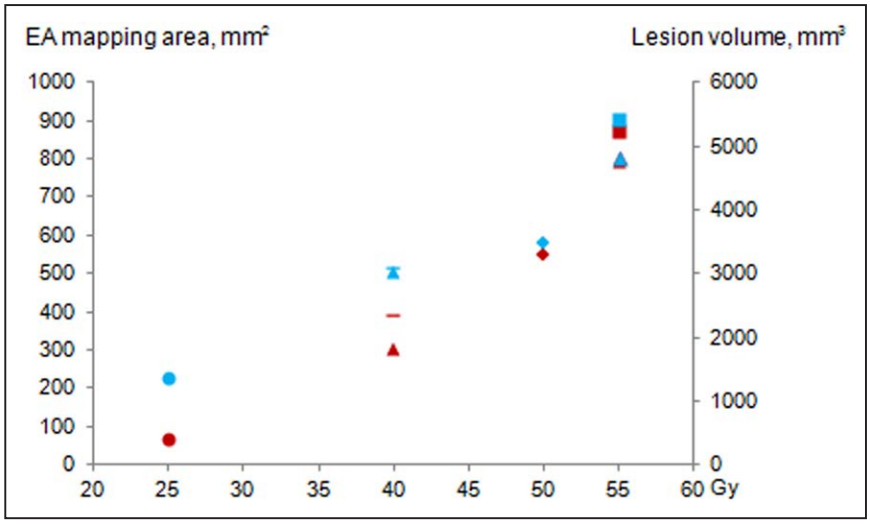

Figure 4. Lesion area from electroanatomical mapping in the right atrium (red markers), plotted along with the calculated macroscopic lesion volume after necropsy (blue markers) against the dose administered to the target volume- One marker symbol represents data for one animal, respectively. Ordinate and abscissa are as labeled.

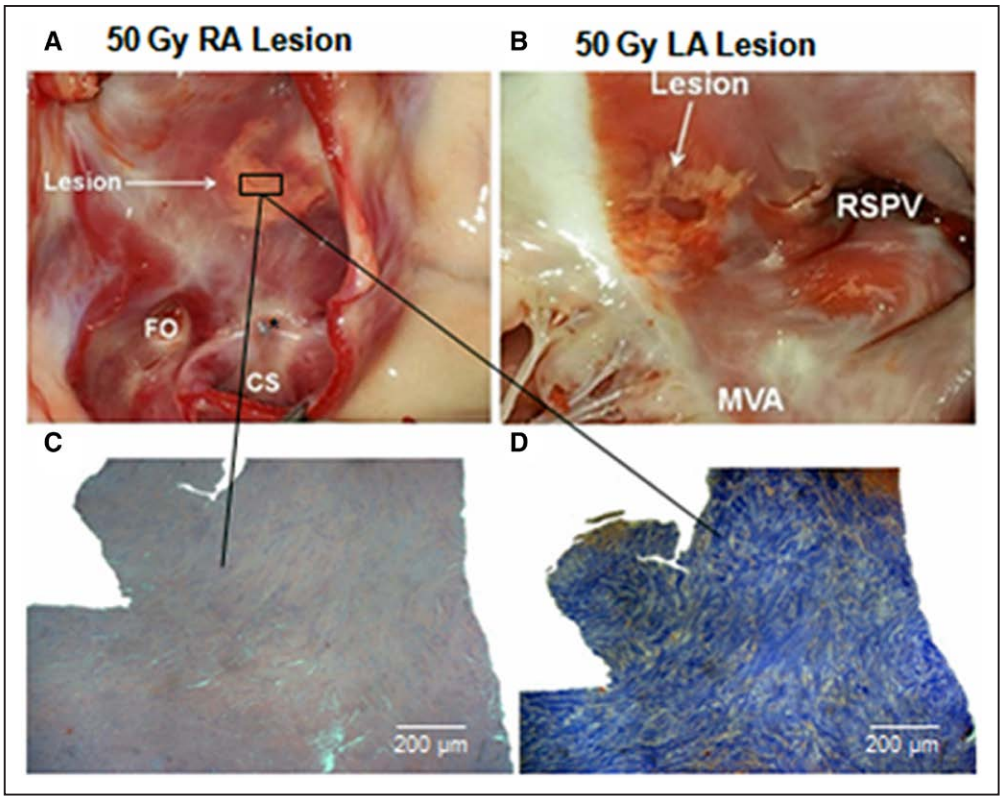

Figure 5. Representative lesion area for atrioventricular junction (AVJ) ablation in the right (**A**) and left atrium (**B**) after irradiation with 50 Gy. The right atrium is opened through the vena cava, and the left atrium is opened over the mitral annulus. Lesions are marked with arrows. Histological cross-sections of the ablation lesion in the triangle of Koch shown in (**C**) hematoxylin and eosin and (**D**) Masson trichrome. CS indicates coronary sinus ostium; FO, fossa ovalis; MVA, mitral valve annulus; and RSPV, right superior pulmonary vein. *Radio-opaque marker.

conducted deliveries for pulmonary vein isolation and ventricular myocardial irradiation in the nonarrhythmic animal model. Success rate of catheter ablation in both diseases is still limited, driving our investigations with photon and particle beam therapies.[15,23,24] The physical properties of photon beams could make these beams an attractive energy source for ablation whenever larger, deeply situated myocardial volumes are treated that do not require extremely sharp energy fall-off and that can neither be reached from the endo- or epicardial surfaces.

Conclusions

This is the first systematic study using several doses of external photon beam therapy for atrioventricular node ablation in intact animals. Using this respective target volume, doses as low as 25 Gy caused electrophysiological and structural myocardial ablation effects. Doses ≥40 Gy created reliable ablation with interruption of cardiac impulse propagation. Targeting (ie, the necessary volume leading to the desired effect), dosing, and long-term cardiac and noncardiac side effects require further investigation for the several different ablation targets and photon versus particle beam sources.

Acknowledgments

Dr Lehmann thanks the American Heart Association and the German Heart Foundation (mit Unterstützung der Deutschen Herzstiftung e.V.) for fellowship funding. All authors would like to thank the therapist team from Mayo Clinic's Department of Radiation Oncology for pertinent help in animal positioning during CT imaging and photon irradiation.

Sources of Funding

Fellowship funding for Dr Lehmann came from the American Heart Association Midwest Affiliate Postdoctoral Fellowship Grants (13POST16810065 and 15POST24800012) and the German Heart Foundation (S03/12; Mit Unterstützung der Deutschen Herzstiftung e.V.). Dr Packer's work is funded in part by a clinician investigator award from the Mayo Foundation. Dr Packer's work is also supported by the Mayo Clinic Foundation development grants and the Goldsmith Foundation as well as the Sanford Diller Foundation.

Disclosures

Dr Packer in the past 12 months has provided consulting services for Abbott Laboratories, Abiomed, Aperture Diagnostics, Biosense Webster, Inc, Boston Scientific, CardioFocus, CardioInsight Technologies, Johnson and Johnson Healthcare Systems, Johnson and Johnson, MediaSphere Medical, LLC, Medtronic CryoCath, Siemens, and St. Jude Medical. Dr Packer received no personal compensation for these consulting activities. Dr Packer receives research funding from the American Heart Association Foundation Award, Biosense Webster, Boston Scientific/EPT, CardioInsight, CardioFocus, Endosense, EpiEP, EP Rewards, Hansen Medical, Medtronic CryoCath LP, NIH, St Jude Medical, Siemens, and Thermedical. Dr Packer also receives royalties from Blackwell Publishing and St. Jude Medical. The other authors report no conflicts.

References

1. Dickfeld T, Tian J, Ahmad G, Jimenez A, Turgeman A, Kuk R, Peters M, Saliaris A, Saba M, Shorofsky S, Jeudy J. MRI-guided ventricular tachycardia ablation: integration of late gadolinium-enhanced 3D scar in patients with implantable cardioverter-defibrillators. *Circ Arrhythm Electrophysiol*. 2011;4:172–184. doi: 10.1161/CIRCEP.110.958744.

2. Soejima K, Stevenson WG, Sapp JL, Selwyn AP, Couper G, Epstein LM. Endocardial and epicardial radiofrequency ablation of ventricular tachycardia associated with dilated cardiomyopathy: the importance of low-voltage scars. *J Am Coll Cardiol*. 2004;43:1834–1842. doi: 10.1016/j.jacc.2004.01.029.
3. Dinov B, Arya A, Bertagnolli L, Schirripa V, Schoene K, Sommer P, Bollmann A, Rolf S, Hindricks G. Early referral for ablation of scar-related ventricular tachycardia is associated with improved acute and long-term outcomes: results from the Heart Center of Leipzig ventricular tachycardia registry. *Circ Arrhythm Electrophysiol*. 2014;7:1144–1151. doi: 10.1161/CIRCEP.114.001953.
4. Soejima K, Suzuki M, Maisel WH, Brunckhorst CB, Delacretaz E, Blier L, Tung S, Khan H, Stevenson WG. Catheter ablation in patients with multiple and unstable ventricular tachycardias after myocardial infarction: short ablation lines guided by reentry circuit isthmuses and sinus rhythm mapping. *Circulation*. 2001;104:664–669.
5. Gerstenfeld EP. Recurrent ventricular tachycardia after catheter ablation in post-infarct cardiomyopathy: "failure" of ablation or progression of the substrate? *J Am Coll Cardiol*. 2013;61:74–76. doi: 10.1016/j.jacc.2012.07.057.
6. Takami M, Lehmann HI, Parker KD, Welker KM, Johnson SB, Packer DL. Effect of left atrial ablation process and strategy on microemboli formation during irrigated radiofrequency catheter ablation in an *in vivo* model. *Circ Arrhythm Electrophysiol*. 2016;9:e003226. doi: 10.1161/CIRCEP.115.003226.
7. Deneke T, Jais P, Scaglione M, Schmitt R, DI Biase L, Christopoulos G, Schade A, Mügge A, Bansmann M, Nentwich K, Müller P, Krug J, Roos M, Halbfass P, Natale A, Gaita F, Haines D. Silent cerebral events/lesions related to atrial fibrillation ablation: a clinical review. *J Cardiovasc Electrophysiol*. 2015;26:455–463. doi: 10.1111/jce.12608.
8. Cappato R, Calkins H, Chen SA, Davies W, Iesaka Y, Kalman J, Kim YH, Klein G, Natale A, Packer D, Skanes A, Ambrogi F, Biganzoli E. Updated worldwide survey on the methods, efficacy, and safety of catheter ablation for human atrial fibrillation. *Circ Arrhythm Electrophysiol*. 2010;3:32–38. doi: 10.1161/CIRCEP.109.859116.
9. Calkins H, Kuck KH, Cappato R, Brugada J, Camm AJ, Chen SA, Crijns HJ, Damiano RJ Jr, Davies DW, DiMarco J, Edgerton J, Ellenbogen K, Ezekowitz MD, Haines DE, Haissaguerre M, Hindricks G, Iesaka Y, Jackman W, Jalife J, Jais P, Kalman J, Keane D, Kim YH, Kirchhof P, Klein G, Kottkamp H, Kumagai K, Lindsay BD, Mansour M, Marchlinski FE, McCarthy PM, Mont JL, Morady F, Nademanee K, Nakagawa H, Natale A, Nattel S, Packer DL, Pappone C, Prystowsky E, Raviele A, Reddy V, Ruskin JN, Shemin RJ, Tsao HM, Wilber D; Heart Rhythm Society Task Force on Catheter and Surgical Ablation of Atrial Fibrillation. 2012 HRS/EHRA/ECAS expert consensus statement on catheter and surgical ablation of atrial fibrillation: recommendations for patient selection, procedural techniques, patient management and follow-up, definitions, endpoints, and research trial design: a report of the Heart Rhythm Society (HRS) Task Force on Catheter and Surgical Ablation of Atrial Fibrillation. Developed in partnership with the European Heart Rhythm Association (EHRA), a registered branch of the European Society of Cardiology (ESC) and the European Cardiac Arrhythmia Society (ECAS); and in collaboration with the American College of Cardiology (ACC), American Heart Association (AHA), the Asia Pacific Heart Rhythm Society (APHRS), and the Society of Thoracic Surgeons (STS). Endorsed by the governing bodies of the American College of Cardiology Foundation, the American Heart Association, the European Cardiac Arrhythmia Society, the European Heart Rhythm Association, the Society of Thoracic Surgeons, the Asia Pacific Heart Rhythm Society, and the Heart Rhythm Society. *Heart Rhythm*. 2012;9:632–696.e21. doi: 10.1016/j.hrthm.2011.12.016.
10. Pérez-Castellano N, Villacastín J, Aragoncillo P, Fantidis P, Sabaté M, García-Torrent MJ, Prieto C, Corral JM, Moreno J, Fernández-Ortiz A, Vano E, Macaya C. Pathological effects of pulmonary vein beta-radiation in a swine model. *J Cardiovasc Electrophysiol*. 2006;17:662–669. doi: 10.1111/j.1540-8167.2006.00462.x.
11. Franceschi F, Bonan R, Khairy P, Dubuc M, Thibault B, Macle L, Talajic M, Roy D, Koutbi L, Virmani R, Guerra PG. Histopathological effects and evolution of transvenous β-radiation applications in right and left atria: an animal study. *Europace*. 2012;14:745–751. doi: 10.1093/europace/eur351.
12. Guerra PG, Talajic M, Thibault B, Dubuc M, Roy D, Macle L, Leung TK, Arsenault A, Harel F, Grégoire J, Bonan R. Beta-radiation for the creation of linear lesions in the canine atrium. *Circulation*. 2004;110:911–914. doi: 10.1161/01.CIR.0000139865.39885.03.
13. Sharma A, Wong D, Weidlich G, Fogarty T, Jack A, Sumanaweera T, Maguire P. Noninvasive stereotactic radiosurgery (CyberHeart) for creation of ablation lesions in the atrium. *Heart Rhythm*. 2010;7:802–810. doi: 10.1016/j.hrthm.2010.02.010.
14. Paul C. Zei JA, Jose Assad M, Edward G, Douglas W, Patrick M, Miguel H, Erick C, Cuathemoc de la P, Thomas F. First-in-man treatment of atrial fibrillation using cardiac radiosurgery. *Heart Rhythm*. 2016;5. Abstract.
15. Lehmann HI, Graeff C, Simoniello P, Constantinescu A, Takami M, Lugenbiel P, Richter D, Eichhorn A, Prall M, Kaderka R, Fiedler F, Helmbrecht S, Fournier C, Erbeldinger N, Rahm AK, Rivinius R, Thomas D, Katus HA, Johnson SB, Parker KD, Debus J, Asirvatham SJ, Bert C, Durante M, Packer DL. Feasibility study on cardiac arrhythmia ablation using high-energy heavy ion beams. *Sci Rep*. 2016;6:38895. doi: 10.1038/srep38895.
16. Okumura Y, Henz BD, Johnson SB, Bunch TJ, O'Brien CJ, Hodge DO, Altman A, Govari A, Packer DL. Three-dimensional ultrasound for image-guided mapping and intervention: methods, quantitative validation, and clinical feasibility of a novel multimodality image mapping system. *Circ Arrhythm Electrophysiol*. 2008;1:110–119. doi: 10.1161/CIRCEP.108.769935.
17. Grimm J, LaCouture T, Croce R, Yeo I, Zhu Y, Xue J. Dose tolerance limits and dose volume histogram evaluation for stereotactic body radiotherapy. *J Appl Clin Med Phys*. 2011;12:3368.
18. Fishbein MC, Meerbaum S, Rit J, Lando U, Kanmatsuse K, Mercier JC, Corday E, Ganz W. Early phase acute myocardial infarct size quantification: validation of the triphenyl tetrazolium chloride tissue enzyme staining technique. *Am Heart J*. 1981;101:593–600.
19. Sharma A, Maguire P, Fajardo L, Wong D, Sumanaweera T, Fogarty T. Non-invasive approach to myocardial ablation: pathology of stereotactic robot targeted high energy x-ray lesions at potential arrhythmia sites. *Heart Rhythm*. 2008;67. Abstract.
20. Sharma A, Maguire P, Sumanaweera T. Non-invasive ablation of the left superior pulmonary vein-left atrial junction using stereotactic focused radiation. *Circulation*. 2007;116:489. Abstract.
21. Sharma A, Maguire P, Wong D, Sumanaweera T, Steele J, Peterson P, Fajardo L, Takeda P, Fogarty T. New non-invasive therapy for cardiac arrhythmias using stereotactic radiosurgery: initial feasibility testing. *Heart Rhythm*. 2007;68. Abstract.
22. Peulen H, Belderbos J, Rossi M, Sonke JJ. Mid-ventilation based PTV margins in stereotactic body radiotherapy (SBRT): a clinical evaluation. *Radiother Oncol*. 2014;110:511–516. doi: 10.1016/j.radonc.2014.01.010.
23. Constantinescu A, Lehmann HI, Packer DL, Bert C, Durante M, Graeff C. Treatment planning studies in patient data with scanned carbon ion beams for catheter-free ablation of atrial fibrillation. *J Cardiovasc Electrophysiol*. 2016;27:335–344. doi: 10.1111/jce.12888.
24. Lehmann HI, Richter D, Prokesch H, Graeff C, Prall M, Simoniello P, Fournier C, Bauer J, Kaderka R, Weymann A, Szabó G, Sonnenberg K, Constantinescu AM, Johnson SB, Misiri J, Takami M, Miller RC, Herman MG, Asirvatham SJ, Brons S, Jäkel O, Haberer T, Debus J, Durante M, Bert C, Packer DL. Atrioventricular node ablation in Langendorff-perfused porcine hearts using carbon ion particle therapy: methods and an *in vivo* feasibility investigation for catheter-free ablation of cardiac arrhythmias. *Circ Arrhythm Electrophysiol*. 2015;8:429–438. doi: 10.1161/CIRCEP.114.002436.

External Arrhythmia Ablation Using Photon Beams: Ablation of the Atrioventricular Junction in an Intact Animal Model

H. Immo Lehmann, Amanda J. Deisher, Mitsuru Takami, Jon J. Kruse, Limin Song, Sarah E. Anderson, Jack T. Cusma, Kay D. Parker, Susan B. Johnson, Samuel J. Asirvatham, Robert C. Miller, Michael G. Herman and Douglas L. Packer

Circ Arrhythm Electrophysiol. 2017;10:
doi: 10.1161/CIRCEP.116.004304
Circulation: Arrhythmia and Electrophysiology is published by the American Heart Association, 7272 Greenville Avenue, Dallas, TX 75231

Print ISSN: 1941-3149. Online ISSN: 1941-3084